

## Competition of various spin states of $\text{LaCoO}_3$

Min Zhuang, Weiyi Zhang, and Naiben Ming

*National Laboratory of Solid State Microstructures and Department of Physics, Nanjing University, Nanjing 210093, China*

(Received 6 August 1997)

The spin-state transition in perovskite  $\text{LaCoO}_3$  has been a controversial topic ever since its discovery. To obtain a better physical understanding of its origin we have studied various magnetically ordered states of an enlarged double cell, including the low-spin state, intermediate-spin state, high-spin state, as well as all combinations among these three states. The calculations were done within the unrestricted Hartree-Fock approximation and the real-space recursion method. The density of states and stability of various states are analyzed as functions of model parameters. Our results show that the ground state of the system depends on the competition between the crystal-field splitting  $Dq$  and the Hund's coupling  $j$ . For a fixed  $j$ , the ground state of the system changes from the low-spin state to the low-spin high-spin ordered state (LS-HS) and finally to the high-spin high-spin antiferromagnetically ordered state as  $Dq$  is weakened. Our study suggests that the spin-state transition at 90 K probably takes place from the low-spin state to the LS-HS ordered state. [S0163-1829(98)03414-6]

### I. INTRODUCTION

The perovskite compound  $\text{LaCoO}_3$  has very interesting magnetic and transport properties.<sup>1-6</sup>  $\text{LaCoO}_3$  is a nonmagnetic insulator at low temperature, and is usually called a low-spin state (LS,  $S=0$ ) because the atomic configuration ( $t_{2g}^6 e_g^0$ ) of  $\text{Co}^{3+}$  ions has no magnetic moment. As temperature increases, the magnetic susceptibility slowly increases and soon reaches a maximum at  $T \approx 90$  K. Above this temperature, the system shows a Curie-Weiss behavior, which is followed by another structural transition at 500 K. Recent neutron-scattering studies<sup>7</sup> suggested that this high-temperature transition is not dominantly magnetic in origin. The transport measurement found that the system changes from an activated semiconductor to a metallic conductor around 400–600 K.<sup>8</sup> The smooth spin-state transition is also reflected in the electron spectra of  $\text{LaCoO}_3$ , where x-ray photoemission measurements revealed that the valence bands at 80 K and 300 K are rather similar and have no significant change.<sup>9-12</sup>

Regarding the nature of the spin-state transition in perovskite  $\text{LaCoO}_3$ , there are two different opinions present in the literature: Most previous studies treat the spin-state transition at 90 K as the transition from the low-spin state to the thermally excited high-spin state,<sup>3</sup> since the high-spin state (HS,  $S=2$ ,  $t_{2g}^4 e_g^2$ ) is only 10–80 meV higher in energy than the low-spin state.<sup>6</sup> Nevertheless, the recent band-structure calculations using the local-density approximation (LDA+ $U$ ) method<sup>13</sup> (where  $U$  is the on-site  $d$ - $d$  Coulomb interaction) and the Hartree-Fock calculations on the multiband lattice model<sup>14,15</sup> have shown that the intermediate-spin state (IS,  $S=1$ ,  $t_{2g}^5 e_g^1$ ) is more stable than the high-spin state. Furthermore, Korotín *et al.*<sup>13</sup> also found that the orbital ordering in the IS state is responsible for the semiconducting nature of the  $\text{LaCoO}_3$  below 500 K. However, controversy still exists since a similar calculation by Mizokawa and Fujimori<sup>14</sup> did not find the orbitally ordered state. Thus, how the spin-state changes with the temperature is still unclear.

As was emphasized by Raccah and Goodenough,<sup>3</sup> more

complex structures of the supercell play an important role in the spin-state transition. They proposed that the LS-HS ordered state may correspond to the insulating state of the system below 400–600 K. More recently, Señaris-Rodríguez and Goodenough<sup>16</sup> have hypothesized the possible states in each temperature domain according to their experimental data. They suggested that the system is in the LS state below 35 K, the LS-HS disordered state between 35 and 110 K, the LS-HS ordered state between 110 and 350 K, and the IS-HS ordered state at a higher temperature above 650 K. Therefore, to obtain a better physical understanding of the spin-state transition in the perovskite  $\text{LaCoO}_3$  and of the origin of the paramagnetic state with local magnetic moments, it is necessary to examine the various spin-ordered states of an enlarged supercell of  $\text{LaCoO}_3$  and study their stability at least around the first spin-state transition.

In this paper, we have studied the various magnetic states of an enlarged double cell of  $\text{LaCoO}_3$ . In addition to the LS, IS, and HS states that were investigated previously, we have also considered all possible combinations among the three states. The calculation is performed within the unrestricted Hartree-Fock approximation on a realistic perovskite-type lattice model and the self-consistent solutions are obtained using the iteration method. With the band-structure parameters deduced from the photoemission spectra as input, our calculated spectra of the low-spin state and the intermediate-spin state, as well as the high-spin state all agree with previous works.<sup>13-15</sup> To compare the relative stability of the various states, we have computed their energies as functions of the crystal-field strength ( $10Dq$ ) and the exchange coupling  $j$  since the phase diagram mainly depends on the competition between these two parameters.<sup>3</sup> Our results show that for a fixed exchange coupling  $j$ , the ground state of the system changes from the LS state to the LS-HS ordered state and finally to the HS-HS antiferromagnetically ordered state (HS-HS-AFM) as the crystal field strength  $Dq$  is weakened. For the parameter range where the LS state is the ground state, the lowest excited state is the LS-HS ordered state. This indicates that the first spin-state transition most likely

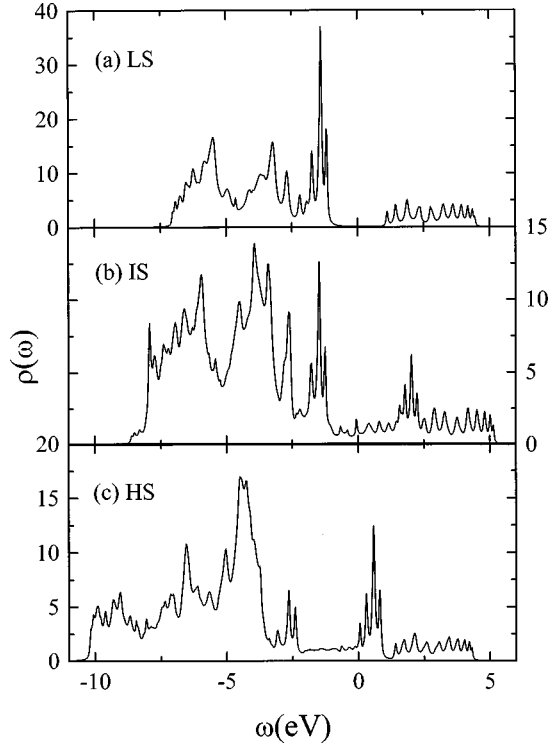


FIG. 1. The total density of states of (a) the LS state, (b) the IS state, and (c) the HS state for  $j=0.84$  eV and  $Dq=0.16$  eV. The other parameters are described in the text.

takes place from the LS state to the LS-HS ordered state, which is in accordance with the phenomenological picture.<sup>16</sup>

The rest of the paper is organized as follows: In Sec. II, we first introduce the perovskite-type lattice model and the unrestricted Hartree-Fock approximation; then real-space recursion method is also briefly outlined. In Sec. III, we present the numerical results and the corresponding discussion for each state. The conclusion is drawn in Sec. IV.

## II. THEORETICAL FORMALISM

The Hamiltonian we start with is the multiband  $d$ - $p$  model,<sup>14</sup> which includes the full degeneracy of the transition metal  $3d$  orbitals and oxygen  $2p$  orbitals as well as on-site Coulomb and exchange interactions:

$$\begin{aligned}
 \mathcal{H} = & \sum_{im\sigma} \epsilon_{dm}^0 d_{im\sigma}^\dagger d_{im\sigma} + \sum_{jn\sigma} \epsilon_p p_{jn\sigma}^\dagger p_{jn\sigma} \\
 & + \sum_{ijmn\sigma} (t_{ij}^{mn} d_{im\sigma}^\dagger p_{jn\sigma} + \text{H.c.}) \\
 & + \sum_{ijn'n'\sigma} (t_{ij}^{n'n'} p_{in\sigma}^\dagger p_{jn'\sigma} + \text{H.c.}) \\
 & + \sum_{im} u d_{im\uparrow}^\dagger d_{im\uparrow} d_{im\downarrow}^\dagger d_{im\downarrow} \\
 & + \frac{1}{2} \sum_{im \neq m' \sigma \sigma'} \tilde{u} d_{im\sigma}^\dagger d_{im\sigma} d_{im'\sigma'}^\dagger d_{im'\sigma'} \\
 & - j \sum_{im\sigma\sigma'} d_{im\sigma}^\dagger \sigma d_{im\sigma'} \cdot \mathbf{S}_{im}^d, \quad (1)
 \end{aligned}$$

where  $d_{im\sigma}$  ( $d_{im\sigma}^\dagger$ ) and  $p_{jn\sigma}$  ( $p_{jn\sigma}^\dagger$ ) denote the annihilation (creation) operators of an electron on a Co  $d$  orbital at site  $i$  and an O  $p$  orbital at site  $j$ , respectively, and  $\epsilon_{dm}^0$  and  $\epsilon_p$  are their corresponding on-site energies.  $m$  and  $n$  refer to the orbital index and  $\sigma$  to the spin. The crystal-field-splitting energy is included in  $\epsilon_{dm}^0$ , i.e.,  $\epsilon_d^0(t_{2g}) = \epsilon_d^0 - 4Dq$  and  $\epsilon_d^0(e_g) = \epsilon_d^0 + 6Dq$ , where  $\epsilon_d^0$  is the bare on-site energy of  $d$  orbital.  $t_{ij}^{mn}$  and  $t_{ij}^{n'n'}$  are the nearest-neighbor hopping integrals for  $p$ - $d$  and  $p$ - $p$  which are related to the Slater-Koster parameters ( $pd\sigma$ ), ( $pd\pi$ ), ( $pp\sigma$ ), and ( $pp\pi$ ).<sup>17</sup>  $\mathbf{S}_{im}^d$  is the total spin operator of a Co ion, extracting the one in orbital  $m$ .  $\tilde{u} = u - 5j/2$ , where the parameter  $u$  is related to the multiplet averaged  $d$ - $d$  Coulomb interaction  $U$  via  $u = U - (20/9)j$ .

In the unrestricted Hartree-Fock approximation, the Hamiltonian becomes linearized and reduces to

$$\begin{aligned}
 \mathcal{H} = & \sum_{im\sigma} \left[ \epsilon_{dm}^0 + u n_{im\sigma}^d - \frac{j}{2} \sigma (\mu_t^d - \mu_m^d) + \tilde{u} (n_t^d - n_m^d) \right] \\
 & \times d_{im\sigma}^\dagger d_{im\sigma} + \sum_{jn\sigma} \epsilon_p p_{jn\sigma}^\dagger p_{jn\sigma} \\
 & + \sum_{ijmn\sigma} (t_{ij}^{mn} d_{im\sigma}^\dagger p_{jn\sigma} + \text{H.c.}) \\
 & + \sum_{ijn'n'\sigma} (t_{ij}^{n'n'} p_{in\sigma}^\dagger p_{jn'\sigma} + \text{H.c.}) \quad (2)
 \end{aligned}$$

Here,  $n_{m\sigma}^d = \langle d_{m\sigma}^\dagger d_{m\sigma} \rangle$ ,  $\mu_m^d = n_{m\uparrow}^d - n_{m\downarrow}^d$ , and  $n_t^d$  and  $\mu_t^d$  are the total electron numbers and magnetization of the Co  $d$  orbitals.

For the tight-binding Hamiltonian, Eq. (2), the density of states can be easily calculated using the real-space recursion method<sup>18</sup> and the Green's function is written as

$$G(\omega) = \frac{b_0^2}{\omega - a_0 - \frac{b_1^2}{\omega - a_1 - \frac{b_2^2}{\omega - a_2 - \frac{b_3^2}{\omega - a_3 - \dots}}}}. \quad (3)$$

The recursion coefficients  $a_i$  and  $b_i$  are obtained from the tridiagonalization of the tight-binding Hamiltonian matrix for a given starting orbital. The multiband terminator<sup>19</sup> is chosen to close the continuous fractional. To study the spin-state transition in LaCoO<sub>3</sub>, we have considered various ordered states of an enlarged double cell of LaCoO<sub>3</sub>. We have computed 25 levels for each of the 38 independent orbitals; the results are checked for different levels and better than 5 meV in energy accuracy is secured. The whole procedure is iterated self-consistently until convergence and the density of states is obtained by  $\rho_{ms}(\omega) = -(1/\pi) \text{Im} G_{ms}(\omega)$ . This allows us to calculate the electron numbers and magnetic moments, as well as the energies of various ordered states.

### III. NUMERICAL RESULTS AND DISCUSSIONS

In this paper, we use the parameter set derived from the cluster model analysis of the photoemission spectra.<sup>14</sup> The bare on-site energies of Co  $d$  and O  $p$  orbitals are taken as  $\epsilon_d^0 = -28.0$  eV and  $\epsilon_p = 0$  eV. The Slater-Koster parameters are  $(pd\sigma) = -2.0$  eV,  $(pd\pi) = 0.922$  eV,  $(pp\sigma) = 0.6$  eV, and  $(pp\pi) = -0.15$  eV, respectively. The on-site Coulomb repulsion is  $U = 5.0$  eV. The crystal-field strength and Hund's coupling are set as  $Dq = 0.16$  eV and  $j = 0.84$  eV. With the parameter set given above, we have studied the electronic structures of various ordered spin states and compared with the experimental observed spectra. Furthermore, to analyze the stability of various ordered spin states, we have calculated their energies as a function of the crystal-field strength for two sets of Hund's coupling  $j = 0.84$  eV and  $j = 0.88$  eV. Our detailed numerical analyses show that the lowest excited state is the LS-HS ordered spin state. Its energy is always lower than the intermediate-spin state in the parameter range where the LS state is the absolute ground state. Thus, our study indicates that the modulated structure is more favorable in energy than the translationally invariant state and disorder effects may play an important role in the spin-state transition of  $\text{LaCoO}_3$ . Below we describe the various ordered states one by one.

In Fig. 1(a), we present the density of states of the low-spin state (LS,  $t_{2g}^6 e_g^0$ ). The Fermi energy ( $E_F \equiv 0$ ) is at the middle of the band gap and LS state is an insulator. There are three major peaks below the Fermi energy. The peak near the top of the valence band comes mostly from the occupied  $t_{2g}$  band; the other two peaks below the Fermi energy are mainly contributed by the O  $p$  orbitals. The  $e_g$  band is located above the Fermi energy and is nearly unoccupied. The occupancy of the  $d$  band is 6.86 which is larger than 6 due to the charge transfer from O  $p$  to Co  $d$  orbitals. These features are in agreement both with the photoemission spectra<sup>9</sup> and with the previous results obtained using the LSDA method.<sup>20</sup> But the gap is overestimated due to the limitation of the Hartree-Fock approximation. As is well known, the Hartree-Fock method gives to the first-order approximation a qualitatively correct result. Better methods such as the slave boson method may change the results quantitatively, but not qualitatively.

The intermediate-spin state (IS,  $t_{2g}^5 e_g^1$ ) as was proposed by Korotin *et al.*<sup>13</sup> is also found in our calculation and is shown in Fig. 1(b). The overall shape of the density of states is quite similar to the LS state except that the  $t_{2g}$  band becomes split due to the presence of a magnetic moment. The magnetic moment and occupancy of the  $d$  orbital are  $2.13\mu_B$  and 6.83, respectively. The IS state is a metal, since the density of states at the Fermi energy is nonzero. It is a metastable state and is 0.19 eV/(per unit cell) higher in energy than that of the LS state. The IS state was proposed as a possible candidate for the state after the 90 K spin-state transition by Korotin *et al.*,<sup>13</sup> but the metallic nature of the IS state is not consistent with the experimental observation. As we will discuss late in the paper, a new LS-HS ordered state has a much lower energy than that of the IS state and it is an insulator.

The next homogeneous solution is the high-spin state (HS,  $t_{2g}^4 e_g^2$ ) which has been widely investigated.<sup>13-15</sup> Its

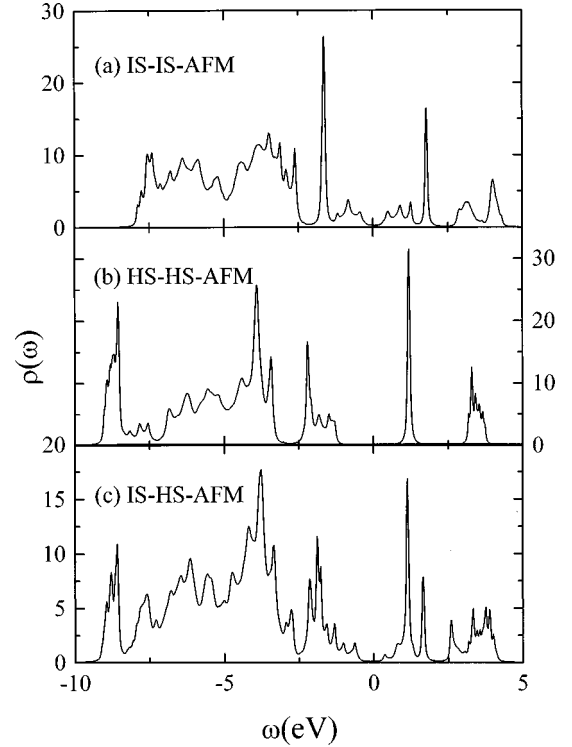


FIG. 2. Same as Fig. 1, but for the total density of states of (a) the IS-IS-AFM state, (b) the HS-HS-AFM state, and (c) the IS-HS-AFM state.

density of states is plotted in Fig. 1(c). The similar features in the densities of states of the IS state and the HS state are mainly contributed by the O  $p$  band. The overall bandwidth is expanded due to the splitting of both the  $t_{2g}$  and  $e_g$  bands. The two peaks just above and below the Fermi energy come from the split  $t_{2g}$  band while the two peaks located at the upper and lower edges are due to the split  $e_g$  band. The HS state is also a metallic state, where its energy is 0.66 eV higher than that of the LS state and 0.47 eV higher than that of the IS state. The magnetic moment of the HS state is  $3.40\mu_B$  and the occupancy of the  $d$  band is 6.54.

Besides the above three spin states which have been investigated previously, we have studied various spin-ordered states of a enlarged double cell of  $\text{LaCoO}_3$ . The first is the (IS-IS-AFM) state where the neighboring IS moments align antiferromagnetically. As can be seen from the density of states shown in Fig. 2(a), the partial density of states of O  $p$  orbitals has a similar shape as that of the LS state, but the Co  $d$  bands are further split due to antiferromagnetic ordering within the double cell. There is an absolute band gap at the Fermi energy and the state is a band insulator. The occupancy of the  $d$  band in this state is similar to the pure IS state, but the local moment  $1.77\mu_B$  is smaller than that of the IS state.

The antiferromagnetically ordered HS state (HS-HS-AFM) is calculated in the same way and its density of states is plotted in Fig. 2(b). The main difference from the HS state comes from the split Co  $d$  bands. This state is also a band insulator with a rather wide gap and the gap does not disappear with the parameters. Note that this state was defined as the HS state by Takahashi and Igarashi.<sup>15</sup> The occupancy and the local moment in this state are 6.58 and  $3.33\mu_B$ , respectively. We will see below that the HS-HS-AFM state be-

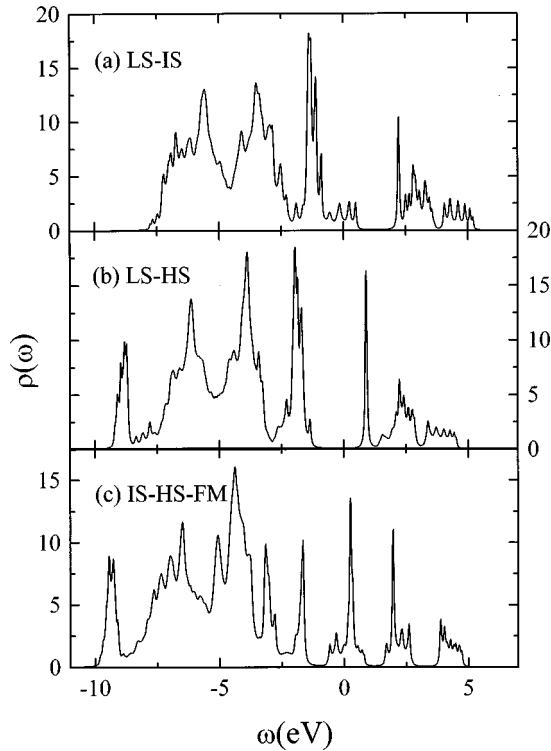


FIG. 3. Same as Fig. 1, but for the total density of states of (a) the LS-IS state, (b) the LS-HS state, and (c) the IS-HS-FM state.

comes the most stable state only for small  $Dq$ , which is not relevant for  $\text{LaCoO}_3$  compound.

The third spin-ordered state is the antiferromagnetically ordered IS-HS state (IS-HS-AFM). From the density of states as plotted in Fig. 2(c), this state can be envisaged as a superposition of the IS-IS-AFM state and the HS-HS-AFM state. There exists an absolute gap at the Fermi energy, but the gap has the same size as that of the IS-IS-AFM state. The energy of this state is lower than that of the IS-IS-AFM state, but higher than that of the HS-HS-AFM state. The occupancy takes the value of 6.81 for the IS site and 6.56 for the HS site; the magnetic moment is  $3.36\mu_B$  for the HS site and  $1.75\mu_B$  for the IS site.

In addition to the antiferromagnetically spin-ordered states as described above, the following three spin-ordered states can be viewed as the direct superpositions of the LS, IS, and HS states. They are the LS-IS ordered state (LS-IS), the LS-HS ordered state (LS-HS), and the IS-HS ferromagnetically ordered state (IS-HS-FM). In Fig. 3(a), the density of states of the LS-IS state is demonstrated and its gross pattern is composed of the LS and IS states. The major structures in the vicinity of the Fermi energy come from the  $t_{2g}$  bands. This state is metallic since there is a nonvanishing density of states at the Fermi energy. The occupancy of the Co  $d$  orbital is 6.93 for the LS site and 6.79 for the IS site. The magnetic moment is  $0.28\mu_B$  for the LS site,  $2.06\mu_B$  for the IS site. Note that the magnetic moment of the LS site becomes nonzero because of hybridization. A similar phenomenon occurs also in the LS-HS ordered state.

The LS-HS state is a band insulator as shown in Fig. 3(b). The analysis of the partial density of states reveals that the peak at the top of the valence band of LS-HS states comes mainly from the  $t_{2g}$  orbitals of the LS Co sites. Therefore,

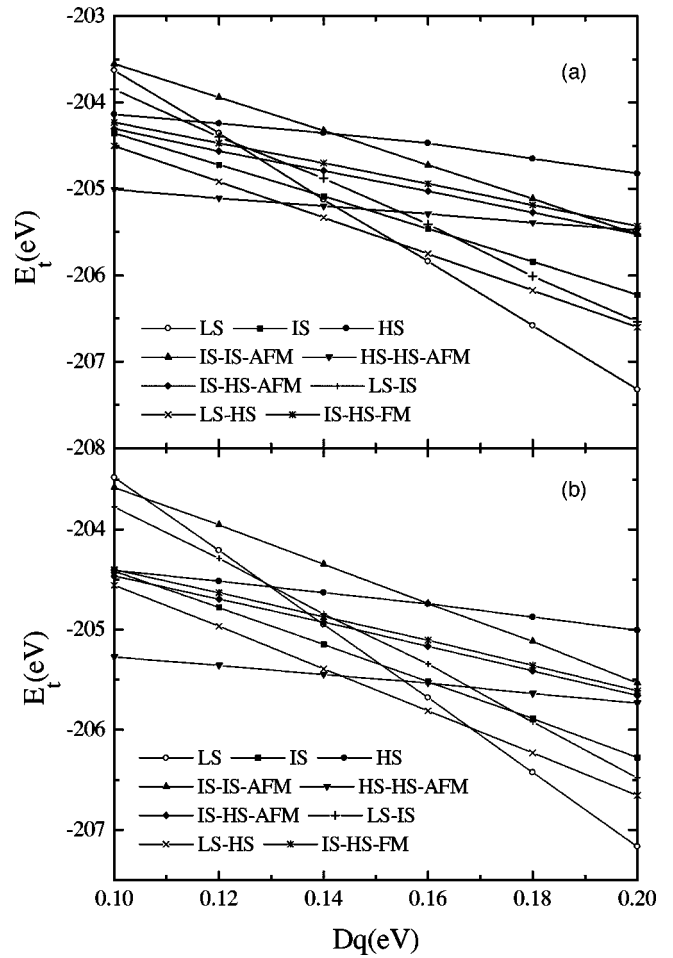


FIG. 4. The energies per unit cell of the various spin states as a function of  $Dq$ . (a)  $j=0.84$  eV and (b)  $j=0.88$  eV. Other parameters are described in the text.

the peak intensity is reduced in comparison with that of the LS state. As we will see below, in the parameter range where the LS state is the absolute ground state, the LS-HS state is the lowest excited state of the system. In particular, this state becomes the first energetically favorable state when the crystal-field strength  $Dq$  is reduced, hence the ground state of the system. The occupancy of the Co  $d$  orbital is 6.94 for the LS site and 6.53 for the HS site; the magnetic moment is  $0.23\mu_B$  for the LS sites and  $3.37\mu_B$  for the HS sites.

The last state we investigated in this paper is the IS-HS ferromagnetically ordered state (IS-HS-FM) which is shown in Fig. 3(c). This state is a hybridized state between the IS and HS states. The binding and antibinding states of the neighboring cells makes a rich structures in the density of states. This state is metallic. The occupancy of the Co  $d$  orbital is 6.81 for the IS sites and 6.56 for the HS sites, the magnetic moment is  $1.75\mu_B$  for the IS site and  $3.36\mu_B$  for the HS site. It is interesting to see that in the last three states, the occupancy and the magnetic moment of each site are much closer to the pure states they are designated, but the total energy and the spectra are very different from one another. The band structures become more complex as the magnetic ordering changes from the LS-IS state to the LS-HS state and finally to the IS-HS-FM state. This trend indicates that the splitting of the band comes from both long-

range ferromagnetical ordering and the magnetic exchange interaction. Note that the little nipple found in some of the densities of states may be due to the limited number of levels used in the recursion routine, but the overall features are correct. This ensures that the quantities, such as local magnetic moments and energy, can be calculated reliably, since they involve an integration over the density of states.

To obtain a better physical understanding of the spin-state transition in the perovskite  $\text{LaCoO}_3$  and of the origin of the paramagnetic state with local magnetic moments, it is necessary to compare the relative stability of all the states above. In Fig. 4, we have calculated energies per unit cell of various spin states as a function of crystal-field strength  $Dq$  for two sets of Hund's coupling  $j=0.84$  eV and  $j=0.88$  eV. The  $Dq$  changes from 0.10 eV to 0.20 eV. Since the Hund's coupling  $j$  and crystal-field strength  $Dq$  affect the energies in a correlated fashion, the energy diagrams for different  $j$  looks the same except for a shift of the horizontal coordinate. For weak crystal-field strength, the HS-HS-AFM ordered state is the ground state of the system; as  $Dq$  increases the LS-HS ordered state becomes energetically more favorable, and the LS state becomes the ground state when  $Dq$  increases further. All three states are a band insulator. Other states we studied are energetically unfavorable as shown in Fig. 4.

For the parameter range which is relevant to the experiments, the LS state is the ground state. We find that the lowest excited state is the LS-HS ordered state. The energy difference between the LS-HS state and the LS state decreases as  $Dq$  decreases. Previous works all concentrated on the LS, IS, and HS states; thus they concluded that the temperature-induced spin-state transition at 90 K takes place between the LS state to the IS state. However, the IS state is much higher in energy than the LS-HS ordered state found in this paper. Actually, the IS state will never become a ground

state in our parameter range. A simple scaling law indicates that the  $Dq$  decreases as temperature increases. Our study suggests that a 90-K spin-state transition probably takes place from the LS state to our LS-HS state.<sup>3,16</sup> Since the energy of the LS-HS state is so close to the ground state, the short-range-ordered LS-HS state may occur well below 90 K and account for the rapid increasing of the magnetic susceptibility.<sup>16</sup>

#### IV. CONCLUSION

In this paper, we have studied the various spin states of an enlarged double cell of  $\text{LaCoO}_3$ . The nine different states are analyzed in detail using the unrestricted Hartree-Fock approximation of the multiband  $d-p$  model and the energy diagrams are obtained as functions of crystal-field strength and Hund's coupling for the parameter range which is relevant to the compound. We find that the LS state is the ground state and the lowest excited state is the LS-HS ordered state. The IS state has much higher energy than the LS-HS state. The energy difference between the LS state and LS-HS state decreases as  $Dq$  decreases and the LS-HS state eventually emerges as the ground state. Since  $Dq$  decreases as temperature increases, we conclude that the spin-state transition at 90 K probably takes place from the LS state to the LS-HS ordered state.

#### ACKNOWLEDGMENTS

The present work is supported in part by the National Natural Science Foundation of China under Grant Nos. NNSF 19677202 and 19674027 and the key research project in "Climbing Program" by the National Science and Technology Commission of China.

- 
- <sup>1</sup>R. R. Heikes, R. C. Miller, and R. Mazelsky, *Physica* (Amsterdam) **30**, 1600 (1964).  
<sup>2</sup>C. S. Naiman, R. Gilmore, B. DiBartolo, A. Linz, and R. Santoro, *J. Appl. Phys.* **36**, 1044 (1965).  
<sup>3</sup>P. M. Raccach and J. B. Goodenough, *Phys. Rev.* **155**, 932 (1967).  
<sup>4</sup>G. H. Jonker, *J. Appl. Phys.* **37**, 1424 (1966).  
<sup>5</sup>V. G. Bhide, D. S. Rajoria, G. R. Rao, and C. N. R. Rao, *Phys. Rev. B* **6**, 1021 (1972).  
<sup>6</sup>K. Asai, P. Gehring, H. Chou, and G. Shirane, *Phys. Rev. B* **40**, 10 982 (1989).  
<sup>7</sup>K. Asai, O. Yokokura, N. Nishimori, H. Chou, J. M. Tranquada, G. Shirane, S. Higuchi, Y. Okajima, and K. Kohn, *Phys. Rev. B* **50**, 3025 (1994).  
<sup>8</sup>S. Yamaguchi, Y. Okimoto, H. Taniguchi, and Y. Tokura, *Phys. Rev. B* **53**, R2926 (1996).  
<sup>9</sup>M. Abbate, J. C. Fuggle, A. Fujimori, L. H. Tjeng, C. T. Chen, R. Potze, G. A. Sawatzky, H. Eisaki, and S. Uchida, *Phys. Rev. B* **47**, 16 124 (1993).  
<sup>10</sup>M. Abbate, R. Potze, G. A. Sawatzky, and A. Fujimori, *Phys. Rev. B* **49**, 7210 (1994).  
<sup>11</sup>A. Chainani, M. Mathew, and D. D. Sarma, *Phys. Rev. B* **46**, 9976 (1992); **47**, 15 397 (1993).  
<sup>12</sup>S. R. Barman and D. D. Sarma, *Phys. Rev. B* **49**, 13 979 (1994).  
<sup>13</sup>M. A. Korotin, S. Yu. Ezhov, I. V. Solovyev, V. I. Anisimov, D. I. Khomskii, and G. A. Sawatzky, *Phys. Rev. B* **54**, 5309 (1996).  
<sup>14</sup>T. Mizokawa and A. Fujimori, *Phys. Rev. B* **53**, R4201 (1996); **54** 5368 (1996); **51** 12 880 (1995).  
<sup>15</sup>M. Takahashi and J. Igarashi, *Phys. Rev. B* **55**, 13 557 (1997).  
<sup>16</sup>M. A. Señaris-Rodríguez and J. B. Goodenough, *J. Solid State Chem.* **116**, 224 (1995).  
<sup>17</sup>J. C. Slater and G. F. Koster, *Phys. Rev.* **94**, 1498 (1954).  
<sup>18</sup>V. Heine, R. Haydock, and M. J. Kelly, in *Solid State Physics: Advances in Research and Applications*, edited by H. Ehrenreich, F. Seitz, and D. Turnbull (Academic, New York, 1980), Vol. 35, p. 215.  
<sup>19</sup>R. Haydock and C. M. M. Nex, *J. Phys. C* **17**, 4783 (1984).  
<sup>20</sup>D. D. Sarma, N. Shanthi, S. R. Barman, N. Hamada, H. Sawada, and K. Terakura, *Phys. Rev. Lett.* **75**, 1126 (1995).